Disturbances of brain cholesterol metabolism: A new excitotoxic process associated with status epilepticus

Aurélie Hanin, Paul Baudin, Sophie Demeret, Delphine Roussel, Sarah Lecas, Elisa Teyssou, Maria Damiano, David Luis, Virginie Lambrecq, Valerio Frazzini, et al.

Disturbances of brain cholesterol metabolism: A new excitotoxic process associated with status epilepticus

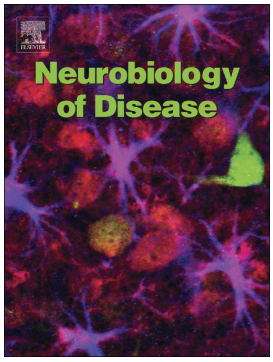

Aurélie Hanin, Paul Baudin, Sophie Demeret, Delphine Roussel, Sarah Lecas, Elisa Teyssou, Maria Damiano, David Luis, Virginie Lambrecq, Valerio Frazzini, Maxens Decavèle, Isabelle Plu, Dominique Bonnefont-Rousselot, Randa Bittar, Foudil Lamari, Vincent Navarro, Morgane Faure, Bastien Herlin, Pierre Jaquet, Clémence Marois, Nicolas Mezouar, Benjamin Rohaut, Nicolas Weiss, Mark Williams, On Behalf of the Study Group

PII: S0969-9961(21)00095-4

DOI: https://doi.org/10.1016/j.nbd.2021.105346

Reference: YNBDI 105346

To appear in: *Neurobiology of Disease*

Received date: 14 January 2021

Revised date: 5 March 2021

Accepted date: 22 March 2021

Please cite this article as: A. Hanin, P. Baudin, S. Demeret, et al., Disturbances of brain cholesterol metabolism: A new excitotoxic process associated with status epilepticus, *Neurobiology of Disease* (2021), https://doi.org/10.1016/j.nbd.2021.105346

Disturbances of brain cholesterol metabolism: a new excitotoxic process associated with status epilepticus

Aurélie Hanin, PharmD[a], Paul Baudin[a], Sophie Demeret, MD[b], Delphine Roussel[a], Sarah Lecas[a], Elisa Teyssou, PhD[a], Maria Damiano, MD, PhD[c], David Luis, MD, MSc[a], Virginie Lambrecq, MD, PhD[a,c,d], Valerio Frazzini, MD, PhD[a,c], Maxens Decavèle, MD[e,f], Isabelle Plu, MD[d,g], Dominique Bonnefont-Rousselot, PharmD, PhD[h,i], Randa Bittar, PharmD[h,j,1], Foudil Lamari, PharmD, PhD[h,1], Vincent Navarro, MD, PhD[a,c,d,k,*] vincent.navarro@aphp.fr, On behalf of the study group

[a]Sorbonne Université, Institut du Cerveau - Paris Brain Institute - ICM, INSERM U 1127, CNRS UMR 7225, Paris, France

[b]AP-HP, Hôpital Pitié-Salpêtrière, DMU Neurosciences 6, Department of Neurology, Neuro-ICU, Paris, France

[c]AP-HP, Hôpital Pitié-Salpêtrière, DMU Neurosciences 6, Epileptology Unit and Clinical Neurophysiology Department, Paris, France

[d]Sorbonne Université, 75006 Paris, France

[e]Sorbonne Université, INSERM, UMRS1158 Neurophysiologie Respiratoire Expérimentale et Clinique, 75005 Paris, France

[f]AP-HP, Hôpital Pitié-Salpêtrière, Service de Pneumologie, Médecine Intensive et Réanimation (Département R3S), Paris, France

[g]AP-HP, Hôpital Pitié-Salpêtrière, DMU Neurosciences 6, Department of Neuropathology, Paris, France

[h]AP-HP, Hôpital Pitié-Salpêtrière, Department of Metabolic Biochemistry, Paris, France

[i]UTCBS, INSERM U 1267, UMR 8258 CNRS, Université de Paris, Paris, France

[j]Sorbonne Université, UMR_S 1166 ICAN, F-75013, Paris, France

[k]Center of Reference for rare epilepsies, Pitié-Salpêtrière Hospital, Paris, France

[*]Corresponding author at: Sorbonne Université, Institut du Cerveau - Paris Brain Institute - ICM, INSERM U 1127, CNRS UMR 7225, Paris, France and AP-HP, Hôpital Pitié-

[1]These authors contributed equally to the manuscript.

Salpêtrière, DMU Neurosciences 6, Epileptology Unit and Clinical Neurophysiology Department, Paris, France. 47-83 Boulevard de l'Hôpital, Paris 75013, France

Abstract

The understanding of the excitotoxic processes associated with a severe status epilepticus (SE) is of major importance.

Changes of brain cholesterol homeostasis is an emerging candidate for excitotoxicity. We conducted an overall analysis of the cholesterol homeostasis both (i) in fluids and tissues from patients with SE: blood (n=63, n=87 controls), CSF (n=32, n=60 controls), and post-mortem brain tissues (n=8, n=8 controls) and (ii) in a mouse model of SE induced by an intrahippocampal injection of kainic acid.

24-hydroxycholesterol levels were decreased in kainic acid mouse hippocampus and in human plasma and post-mortem brain tissues of patients with SE when compared with controls. The decrease of 24-hydroxycholesterol levels was followed by increased cholesterol levels and by an increase of the cholesterol synthesis. Desmosterol levels were higher in human CSF and in mice and human hippocampus after SE. Lanosterol and dihydrolanosterol levels were higher in plasma from SE patients.

Our results suggest that a CYP46A1 inhibition could occur after SE and is followed by a brain cholesterol accumulation. The excess of cholesterol is known to be excitotoxic for neuronal cells and may participate to neurological sequelae observed after SE. This study highlights a new pathophysiological pathway involved in SE excitotoxicity.

Keywords

24-hydroxycholesterol – Cholesterol – Status epilepticus – Excitotoxicity

Abbreviations

24-OHc	24-hydroxycholesterol
25-OHc	25-hydroxycholesterol
ABC	ATP-binding cassette
AED	antiepileptic drug
ApoA1	apolipoprotein A1
ApoE	apolipoprotein E
ARDS	acute respiratory distress syndrome
BBB	blood-brain barrier
CI	confidence intervals
CONT	controls
EC	esterified cholesterol
EPI	epileptic patients
f	female
FC	free cholesterol
FCONT	functional controls
HDL-c	HDL-cholesterol
HMG-CoA	3-hydroxy-3-methylglutaryl coenzyme A
Hpc	hippocampus
ICU	intensive care unit
KA	kainic acid
LDL	Low-density lipoprotein
Lp-PLA2	lipoprotein-associated phospholipase A2
LXR	Liver X receptor
m	male
NORSE	new-onset refractory status epilepticus
NRSE	non-refractory status epilepticus
PBS	phosphate-buffered solution
PSRSE	prolonged super-refractory status epilepticus
RSE	refractory status epilepticus
SD	standard deviation
SE	status epilepticus
SEM	standard error of the mean
TC	total cholesterol
TG	triglycerides
UPLC-MS/MS	ultra-performance liquid chromatography-tandem mass spectrometer.

1. Introduction

Status epilepticus (SE) is a life-threatening prolonged epileptic seizure (Trinka et al., 2015). In 25% of cases, SE is refractory (RSE) to antiepileptic drugs (AED) and requires anesthetics (Rossetti and Lowenstein, 2011). The excessive and sustained activation of neurons can induce excitotoxic processes. As a result, patients may present brain atrophy on MRI, especially in hippocampal structures, with subsequent severe neurologic sequelae, such as cognitive disorders (memory impairment) and a further development of epilepsy (Rossetti et al., 2006).

The understanding of the pathophysiological mechanisms underlying the excitotoxic processes is crucial to better manage the SE by identifying new neuroprotective therapeutics and prevent neurological sequelae that may impact the patient's life quality. We focused on an emerging pathway, the brain cholesterol homeostasis (de Freitas et al., 2010). Brain cholesterol plays a major role in brain development, synaptogenesis and neuronal activity by inhibition or potentiation of voltage-dependent and ligand-gated ion channels activity (Björkhem and Meaney, 2004; Dietschy and Turley, 2004; Korinek et al., 2015; Levitan et al., 2014). Brain cholesterol is synthetized *de novo*, mostly by astrocytes through the Bloch pathway and to a lesser extent in neurons through the Kandutsch-Russel pathway (Mitsche et al., 2015; Zhang and Liu, 2015). Then, cholesterol is transported by apolipoprotein E (ApoE) to neurons. Cholesterol can't freely cross the intact blood-brain barrier (BBB) (Dietschy and Turley, 2004). Cholesterol is metabolized into 24-hydroxycholesterol (24-OHc) by the neuron-specific cholesterol-24 hydroxylase enzyme, encoded by the *CYP46A1* gene (Björkhem et al., 1998; Ramirez et al., 2008). In contrast to cholesterol, 24-OHc can be exported across the BBB and regulates the synthesis and the transport of cholesterol by a negative feedback (Leoni and Caccia, 2013).

Disturbances in brain cholesterol homeostasis were reported in neurodegenerative disorders where excitotoxicity plays a major role (Boussicault et al., 2016; Djelti et al., 2015; Martins et al., 2009). Especially, brain cholesterol accumulation, secondary to CYP46A1 downregulation, was found excitotoxic and responsible of neuronal death (Boussicault et al., 2016; Djelti et al., 2015; Martins et al., 2009). We also reported that blocking CYP46A1 expression in mouse hippocampus resulted in cholesterol accumulation, secondary epileptic abnormalities and progressive neuronal loss (Chali et al., 2015). These cellular and electrographic changes were similar to those observed: (i) in patients who presented with a RSE after the control of the SE and (ii) in animal models of SE two weeks after the induction of SE by kainic acid (KA). It suggests that disturbances in brain cholesterol homeostasis may

occur during SE and participate to the excitotoxic processes. Especially, we wondered if a CYP46A1 inhibition may occur during SE, and be followed by a decrease of 24-OHc levels and accumulation of cholesterol.

Preliminary data on changes of sterol levels in rodents treated by KA are conflicting (Chali et al., 2019; Heverin et al., 2012; Kim et al., 2010; Ong et al., 2010). This may be explained by the large variabilities in methodological processes: different time point assessments and different anatomical sources. The relation between brain and peripheral compartments were rarely studied. To date, the brain cholesterol homeostasis has never been explored in SE patients.

For the first time we aim to characterize the changes in sterol levels both in SE patients and in KA mouse model of SE. To study the kinetic changes, we evaluated sterol levels at different time points after SE onset. In addition, to assess the relationship between the brain and the peripheral compartments, we performed analysis in blood, CSF and brain tissues.

Firstly, we investigated if a CYP46A1 inhibition occurs after SE and if it is followed by a decrease of 24-OHc levels.

Secondly, as 24-OHc regulates cholesterol synthesis, we studied the impact of decreased 24-OHc levels on brain and peripheral cholesterol synthesis.

Thirdly, we studied several ways of exchange between the brain and the peripheral compartments, such as blood-brain barrier permeability, and lipid transport.

2. Materials and methods

2.1. Human fluid study

2.1.1. Study design, settings and participants

We prospectively enrolled both men and women patients from intensive care unit (ICU) and neurology units of Pitié-Salpêtrière Hospital, from February 2013 to May 2019. The protocol was approved by our local (2012, CPP Paris-VI) and by the INSERM ethic committees (C16-16, 20152482). Patients or relatives were informed and no one has opposed. The study design and report are in accordance with the STROBE statement (Cuschieri, 2019).

We included patients aged of 16 years or over and admitted to ICU with an ongoing SE. SE was diagnosed according to the International League Against Epilepsy (Trinka and Kälviäinen, 2017). Patients with post-anoxic SE or with an associated neurodegenerative disease were excluded. SE patients were divided into three groups: non-refractory status epilepticus (NRSE), refractory status epilepticus (RSE) and prolonged super refractory status epilepticus (PSRSE) (Hirsch et al., 2018). RSE is defined as a failure of at least two appropriately selected and dosed parenteral medications including a benzodiazepine, with no specific seizure duration required (Hirsch et al., 2018). PSRSE is defined as a RSE that persists for at least 7 days, including ongoing need for anesthetics (Hirsch et al., 2018).

We included control patients (CONT), who were hospitalized in neurology units of Pitié-Salpêtrière Hospital, aged of 16 years or over. They were divided into two groups: (i) *functional* controls (FCONT) if they had functional neurological disorder, based on normality of clinical examination and lumbar puncture, and (ii) *epileptic* controls (EPI) including patients with epilepsy but no SE. Patients with a neurodegenerative disease were also excluded.

2.1.2. Variables

The primary objective was to characterize the cholesterol homeostasis disturbances related to SE with regards to blood, CSF and brain tissues. Venous blood and CSF samples were drawn to measure lipid parameters, hydroxycholesterols, FC and cholesterol synthesis precursors levels with protocols described below. Analyses were performed on blood from 63 SE patients and 87 CONT. Lumbar punctures were only done for diagnostic purpose and concerned 32 SE patients and 60 CONT (Fig.1).

2.1.3. Study size

This is the first human study conducted to evaluate brain cholesterol homeostasis disturbances induced by SE. Nevertheless, on the basis of animal literature, we estimated that SE patients were four times more likely to present disturbances in lipid homeostasis (OR=4) and those disturbances could be observed in 10% of control patients. Therefore, a total sample size of 136 participants was required for the study (alpha=5%, beta=20%). An interim analysis showed a higher rate of the endpoint than expected (OR=4.5), which reduced the required sample size to 112 participants.

2.2. Human tissues extract

Post-mortem human frozen samples and paraffin tissues of hippocampus, lateral temporal cortex and frontal cortex were obtained from eight controls with no history of acute neurological or psychiatric disorders (delay post death=33 hours), and eight patients with SE diagnosed clinically or based on EEG (delay post death=48 hours). The Table1 gives patient's gender and age, delay of examination post death, cause of death and which frozen and/or paraffin tissues were available for each patient.

2.3. Mouse model of epilepsy

All experimental studies were performed in accordance with the European Committee Council Directive (2010/63/UE) and approved by the local ethics committee (A75-13-19; 8302-2017). Experiments were performed on C57BL/6J male mice, aged of 2 months of age and weighing 20-25g (n=99).

2.3.1. Kainate injection and intracranial surgery

Mice were anesthetized with 2-4% isoflurane performed with analgesia (Buprecare) and placed in a stereotaxic frame. Kainic acid (KA, 50nL; 20mM in PBS) or phosphate-buffered-solution (PBS, 50nL) for control mice, were injected into the right hippocampus (anterior-posterior, -1.8mm; medio-lateral, -1.8mm; dorso-ventral, -1.8mm, with respect to the bregma). This site corresponds to distal dendritic regions of CA1 pyramidal cells (Le Duigou et al., 2008). After injection, 7 mice (2 PBS, 5 KA) were directly implanted with two bipolar stainless-steel electrodes inserted respectively into the right and left hippocampus. A reference electrode was placed on the cerebellum of each mouse. All coordinates were derived and adjusted from Paxinos and Watson mice brain atlas (Paxinos et al., 1985).

2.3.2. Video-EEG recordings

Implanted mice were freely moving and connected to an ADC amplifier, part of a video-EEG acquisition system (Deltamed, Natus). EEG signals were acquired at 4096Hz and band pass filtered (0.5-70Hz). Continuous video-EEG recordings were performed during 72 hours after surgery, then at 6-7 days and at 14-15 days after surgery. Signal analyses were achieved using Deltamed software.

2.3.3. Mice brain tissues preparation

Animals were euthanized, at 1, 3, 7 or 15 days after KA-injection or PBS-injection, by an intraperitoneal injection of pentobarbital. For biochemical analyses, ipsi- and contralateral

hippocampus (n=26 KA-injected mice and n=26 PBS-injected mice; 6 mice per group at 3 and 7 days and 7 mice per group at 1 and 15 days) were dissected. For immunohistochemistry studies, mice (n=20 KA-injected mice and n=20 PBS-injected mice; 5 mice per group, per time) were perfused intracardially with 4% paraformaldehyde.

2.4. Histology and immunohistochemistry

Mouse and human post-mortem brain slices were washed in PBS, and exposed to citrate buffer and Triton. Primary antibodies were applied overnight at 4°C (NeuN, 1:500, MAB377 Merck-Millipore; CYP46A1, 1:500, ab82814 abcam). Secondary antibodies were applied for 1-hour at room temperature (Alexa fluor-555-donkey-anti-mouse, 1:500 for NeuN; Alexa fluor-488-donkey-anti-rabbit, 1:500 for CYP46A1). Images were acquired with Zen software (Zeiss) and fluorescence intensities were quantified using ImageJ software (NIH).

2.5. Biochemical analyses for hydroxycholesterols and cholesterol precursors

Human and mouse tissues were put in an HEPES buffer and homogenized. Homogenates were centrifuged and supernatants were collected. Sterol concentrations were normalized by total protein concentration, evaluated by the bicinchoninic acid assay (Sigma-Aldrich).

An ultra-performance liquid chromatography-tandem mass spectrometer (UPLC-MS/MS) with isotopic dilution method was used to measure hydroxycholesterols (24-hydroxycholesterol and 25-hydroxycholesterol) in plasma, CSF and homogenate brain tissues (Marelli et al., 2018). A similar protocol was applied for sterols (cholesterol, lanosterol, dihydrolanosterol and desmosterol) measurements, with an incubation at room temperature during 45-min.

We measured sitosterol levels, by UPLC-MS/MS, to assess BBB permeability. Sitosterol is a plant sterol only provided *via* food uptake which was proposed to reflect BBB integrity (Heverin et al., 2004; Saeed et al., 2015).

2.6. Lipid parameters

Venous blood samples were collected and centrifuged to obtain serum. Total cholesterol (TC), triglycerides (TG), HDL-cholesterol (HDL-c) were analyzed by enzymatic methods and apolipoprotein A1 (ApoA1) and apolipoprotein B100 (ApoB) by immunoturbidimetric method on Cobas analyzer (Roche). Free cholesterol (FC) was analyzed by colorimetric method on Konelab 30i analyzer (Thermo Fisher Scientifics). Esterified cholesterol (EC) was

calculated by difference (EC=TC-FC). Apolipoprotein E (ApoE) was measured by immunonephelemetric method on BNII analyzer (Siemens).

2.7. ApoE phenotyping

ApoE isoforms were identified with the Hydragel 18 ApoE Isofocusing (Sebia). A ready-to-use agarose gel containing ampholytes was used to perform a semi-automatic electrophoresis, followed by a specific immunofixation, on Hydrasys2 scan instrument(Bittar et al., 2020). Isoforms bands were compared to specific controls.

2.8. Western-blot analyses

Human post-mortem frozen tissues were homogenized in a Tris buffer, completed with a protease inhibitor and a benzonase nuclease and incubated at 37°C for 30-min. Sodium dodecyl sulfate was added to 2%. Protein extracts were centrifuged and supernatants protein concentration was evaluated using the bicinchoninic acid assay. Proteins were separated on NuPAGE^{TM} Bis-Tris Gel (Thermo Fisher Scientific) and electrophoretically transferred to nitrocellulose membranes (PROTAN^{TM} Whatman Gmbh). Primary antibody against CYP46A1 (1:1000) was applied over 3-hours and secondary antibody (1:5000) over 1-hour at room temperature. Signals were detected using ECL^{TM} Prime Western Blotting Detection Reagent (GE Healthcare). Signal intensities were analyzed, on a blinded fashion, with MultiGauge 3.0 software. CYP46A1 concentrations were found by densitometry analysis.

2.9. Statistical analysis

Analyses were performed with R Software (R.3.5.0).

We first performed one-way ANOVA tests to evaluate subgroups impact. Then, pairwise comparisons were performed using Student, Mann-Whitney, or Chi^2 tests when appropriate. The sequential rejective Benjamini-Hochberg test procedure was used to correct for multiple comparisons. Shapiro-Wilk test was performed to assess normality of data distribution. Correlations were evaluated calculating respective Spearman's rho values and their level of significance. Results were considered significant when $P<0.05$.

3. Results

3.1. Study participants

The number of patients for each subgroup and each biological compartment are summarized in Fig.1. Main demographic and biological characteristics are summarized in Table2. NRSE patients were included more quickly after SE onset than those with RSE (P=0.028).

3.2. Time course of epileptic activities and neuronal death in mice after KA injection

3.2.1. Electrophysiological features

Following KA injection, EEG recordings showed SE, defined by intermittent seizures without recovery of normal background between successive seizures, which began after 30-min and lasted for 3 days (Fig.2A-B). At 6-7 days post-injection, we observed an interictal activity including spike-and-wave discharges in both hippocampi. After 2 weeks, we observed spontaneous clonic seizures followed by prolonged postictal depression with EEG flattening (Fig.2A-B).

3.2.2. Histological analyses

A severe progressive neuronal loss was seen in CA1 region (Fig.2C), starting at the 3rd day and almost total at the 15th day (Fig.2D).

3.3. SE induces a decrease of 24-OHc levels both in humans and mice

3.3.1. 24-OHc levels in human post-mortem brain tissues

24-OHc levels were measured in subiculum, lateral temporal cortex and frontal cortex from frozen extracts of post-mortem patients (SE patients n=2, CONT n=3), and normalized by CYP46A1 concentration. In subiculum, we found a higher 24-OHc/CYP46A1 ratio for one patient when compared with CONT (Fig.3A). This patient died after 106 days of a New Onset Refractory Status Epilepticus (NORSE, new onset refractory status epilepticus without a clear acute or active structural, toxic or metabolic cause in a patient without active epilepsy or other preexisting relevant neurological disorder (Hirsch et al., 2018)) and presented with hippocampal atrophy at brain examination. In contrast, there was a decrease of the ratio for the second patient who died only 9 days after SE onset and also suffering from a NORSE (Fig.3A). In temporal cortex and frontal cortex, we found decreased ratio for both patients (Fig.3B-C).

3.3.2. 24-OHc levels in human plasma and CSF

We measured 24-OHc levels in CSF and plasma of CONT and SE patients (Table2). No significant change in CSF 24-OHc levels were found in SE patients, as compared to CONT. However, plasma 24-OHc levels were significantly lower in SE patients when compared with CONT (P=0.00064), FCONT (P=0.018) and EPI (P=0.00087). No difference was found between FCONT and EPI (P=0.25), suggesting that reduced 24-OHc levels are not related to sporadic seizures (Fig.3D). Among SE patients, only NRSE patients had significantly reduced 24-OHc levels when compared with CONT (P<0.001). NRSE patients showed also lower 24-OHc levels than RSE patients (P=0.043) (Fig.3D). In contrast to 24-OHc, we found increased 25-hydroxycholesterol (25-OHc) plasma levels for SE patients when compared with FCONT (P=0.043). RSE patients showed also higher 25-OHc levels than CONT patients (P=0.035) (Fig.3E). We studied the relationship between plasma 24-OHc levels and the time between SE onset and blood sampling: patients who were enrolled quickly after SE onset had significantly lower 24-OHc levels, than those enrolled later (rho=0.25; P=0.047) (Fig.3F).

3.3.3. 24-OHc levels in the hippocampus of KA-induced SE mice

We then measured 24-OHc levels both in ipsilateral and contralateral hippocampi from KA mice. Levels were normalized by the total protein concentration, and expressed as the ratio of 24-OHc levels for KA mice and for PBS mice (Fig.3G). We observed a significant decrease of the ratio the first day after injection in the ipsilateral hippocampus (P=0.047). At the third day, ratios were decreased in ipsilateral (P=0.0015) and contralateral hippocampi (P=0.047). There was no difference between KA and PBS mice during the latent period (D7) and at the time of spontaneous seizures (D15). Decreased 24-OHc levels in KA mice preceded the decrease in NeuN+ cells (Fig.2D), indicating that the reduced 24-OHc production by the CYP46A1 is not merely related to the neuronal death.

3.3.4. CYP46A1 expression levels in human post-mortem brain tissues

As we found decreased 24-OHc levels, we studied the expression of the CYP46A1. In CONT post-mortem tissues (n=3), we found CYP46A1 expression in all cell bodies of subiculum pyramidal cells (Fig.3H). In post-mortem tissues from SE patients (n=7), we did not identify changes in the intensity or the localization of CYP46A1 fluorescence (Fig.3H).

Then, we analyzed CYP46A1 protein expression levels in humans' frozen post-mortem subiculum (CONT n=3, SE patients n=2), lateral temporal cortex (CONT n=8, SE patients

n=2) and frontal cortex (CONT n=8, SE patients n=2). Immunoblots of CYP46A1 showed no significant modifications in CYP46A1 levels in subiculum, lateral temporal cortex and frontal cortex of SE patients when compared with CONT (Fig.3I).

3.4. SE induces an abnormal increase in brain cholesterol synthesis

As our previous results suggest a functional blockage of the CYP46A1, we then studied the substrate of this enzyme: the cholesterol and its precursors. Cholesterol synthesis from acetyl-CoA requires a lengthy biosynthesis and two parallel pathways: the Bloch pathway—which involves desmosterol synthesis—and the Kandutsch-Russel pathway—which involves dihydrolanosterol synthesis (Fig.4A).

3.4.1. Sterol levels in human post-mortem brain tissues

We first measured sterol levels in the homogenates of subiculum, lateral temporal cortex and frontal cortex extracts. We found increased cholesterol and desmosterol levels in the subiculum of SE patients when compared with CONT (Fig.4B). Levels were higher for the patient who had a lower 24-OHc/CYP46A1 ratio (Fig.3A). In the temporal cortex, we found no modification in cholesterol levels for SE patients when compared with CONT (Fig.4C). Nevertheless, as observed in the subiculum, we found increased desmosterol levels in SE patients (Fig.4C). Similar results were obtained in the frontal cortex (Fig.4D). No modification was found for lanosterol and dihydrolanosterol levels (data not shown).

3.4.2. Sterol levels in human CSF

Sterol levels were then measured in CSF from CONT and SE patients (Fig.4E-G). CSF cholesterol levels were increased in SE patients when compared with CONT (P=0.036) (Fig.4E). To identify the synthesis pathway, we measured desmosterol and dihydrolanosterol levels. No modification of dihydrolanosterol levels was found (Fig.4F), while a significant increase of desmosterol levels was observed for SE patients when compared with CONT (P=0.0027) (Fig.4G).

3.4.3. Sterol levels in mice KA model hippocampus

Next, sterol levels were measured in ipsilateral and contralateral hippocampi from KA and PBS mice (Fig.4H-I). We observed a progressive increase in KA/PBS desmosterol ratios with a peak at 3 days (1.68, P=0.015) for the contralateral hippocampus and at 7 days (1.45, P=0.025) for the ipsilateral. We also observed a progressive increase in KA/PBS cholesterol

ratio with a peak at 7 days (P=0.15) (Fig.4I). No modification was found for lanosterol and dihydrolanosterol levels (data not shown).

Altogether these data indicate that SE induces an abnormal increase of brain cholesterol synthesis through the Bloch pathway.

3.5. SE induces disturbances in peripheral cholesterol homeostasis

3.5.1. Total cholesterol, free cholesterol and esterified cholesterol

SE patients had significantly lower total cholesterol (TC) levels when compared with CONT patients (P<0.001). No difference was found between levels of FCONT and EPI (Fig.5A). TC levels were lower for NRSE patients and PSRSE patients. Nevertheless, TC decrease hides different trends from the two subtypes of cholesterol: the free or unesterified cholesterol (FC), which is metabolically active, and the esterified cholesterol (EC), an inactive form stored in the liver. SE patients had lower EC levels when compared with CONT patients (P<0.001). Notably, EC levels were lower for NRSE patients and PSRSE patients when compared to FCONT and EPI (Fig.5B). The cholesterol esterification ratio, obtained as EC/TC, was also lower for SE patients (P<0.001). In contrast, FC levels tend to rise in SE patients, especially for PSRSE patients (P=0.055). We also observed a correlation between serum FC levels and the time between SE onset and blood sampling (rho=0.44; P<0.001) (Fig.5C).

3.5.2. Lipoproteins and apolipoproteins

We then studied changes in the lipid complexes. SE patients showed a decrease of HDL-c levels which was even stronger if SE was sustained (P=0.020 for RSE patients *versus* FCONT; P<0.001 for PSRSE patients *versus* FCONT and RSE patients) (Fig.5D). Contrary to HDL-c, triglyceride levels increased in SE patients (P=0.0016 for PSRSE patients *versus* CONT and P=0.019 for PSRSE patients *versus* RSE patients). No correlation was observed between HDL-c and triglyceride levels (up to 2.5 g/L) in SE patients, indicating that lower HDL-c levels were not merely related to high triglyceride levels (Fig.5E). ApoA1 levels were decreased in SE patients when compared with CONT (P<0.001). No significant change was observed for ApoB levels.

3.5.3. Sterol levels in human plasma

The increase of FC levels could be linked to an increase of lanosterol (P=0.04) (Fig.5F), and dihydrolanosterol (P=0.0076) (Fig.5G) levels in PSRSE patients when compared with CONT. In contrast to the brain findings, no modification in desmosterol levels was found in plasma of SE patients (Fig.5H).

Altogether these data indicate that SE induces an abnormal increase of peripheral cholesterol synthesis through the Kandutsch-Russel pathway and disturbs cholesterol and lipoproteins homeostasis.

3.6. Blood – brain handover in SE

In order to understand relationship between the brain and the peripheral compartments, we further studied several ways of communication between them.

3.6.1. Blood-brain barrier permeability

To study BBB integrity, we measured sitosterol levels in humans and mice. SE patients showed increased CSF sitosterol levels when compared with CONT patients (P=0.0019) (Fig.6A), and an increased percentage of diffusion through the BBB (i.e. $[Sitosterol]_{CSF}/[Sitosterol]_{CSF+plasma}$) ($P<0.001$). Moreover, hippocampus sitosterol levels were doubled, one day after injection, in KA mice when compared with control animals (P=0.029) (Fig.6B).

3.6.2. Lipid transport and ApoE

As ApoE is involved in the lipid transport from liver to peripheral compartments and from astrocytes to neurons, we measured its serum and CSF levels in patients. CSF ApoE levels tend to decrease in SE patients when compared with CONT (P=0.15) (Fig.6C). SE patients showed significantly higher serum ApoE levels when compared with CONT (P=0.0016). We observed increased serum ApoE levels with SE duration (Fig.6D). In addition, we observed a trend to an increase of hippocampal ApoE+ cells 7 days after KA injection (data not shown). Altogether these data suggest an increase of ApoE brain levels.

We further phenotyped ApoE in SE patients and CONT patients (Fig.6E). The E3/E3 phenotype was the most common both in SE patients (63%) and CONT (73%) (Fig.6F). We did not observe any difference between phenotype frequencies in both groups.

4. Discussion and Conclusions

The availability of metabolites measurable in brain, blood or CSF may facilitate the understanding of cellular changes that occur during SE and the implementation of further prospective therapeutic studies. Even if several fluid biomarkers were proposed in SE, none have yet been validated for clinical use (Hanin et al., 2020).

Disturbances in brain cholesterol homeostasis were reported in several neurological disorders such as Alzheimer's disease (Djelti et al., 2015; Martins et al., 2009) or Huntington's disease (Boussicault et al., 2016) and suggested in SE animal models (Chali et al., 2019; Heverin et al., 2012; Kim et al., 2010; Ong et al., 2010). Nevertheless, findings were conflicting and brain cholesterol homeostasis has never been explored in SE patients. We therefore aimed to evaluate more accurately brain cholesterol homeostasis disturbances induced by SE in both patients and animal model.

4.1. CYP46A1 expression is maintained but 24-OHc levels decrease during SE

We did not observe a decrease of CYP46A1 expression in the brain of patients with SE (Fig.3H-I). Nevertheless, in lines with previous studies conducted on neurodegenerative diseases, we observed two-step changes of 24-OHc levels—an initial decrease (Leoni et al., 2008; Solomon et al., 2009), followed by an increase (Lütjohann et al., 2000).

Indeed, the 24-OHc/CYP46A1 ratio was lower than that of controls in subiculum for the patient who died early (9 days) after SE onset (Fig.3A). We observed decreased 24-OHc levels in mouse hippocampi, 1 and 3 days after KA injection (Fig.3G), as well as in plasma from patients who were enrolled shortly after SE onset (Fig.3D-F). SE may induce a CYP46A1 functional inhibition, possibly related to (i) a dysfunction of the CYP46A1 intracellular transfer between endoplasmic reticulum and membranes (Sodero et al., 2012), (ii) an increased requirement for brain cholesterol after injury or (iii) a protective mechanism against 24-OHc neurotoxicity (Noguchi et al., 2015, 2014; Paul et al., 2013; Yamanaka et al., 2011). Decreased 24-OHc production could induce an increased production of 25-OHc, *via* an alternative way of hydroxylation. Increased levels of 25-OHc are involved in inflammation pathways (Pokharel et al., 2019) and may participate to SE excitotoxicity. No difference of 24-OHc levels was found in CSF. Measurement of 24-OHc in CSF was previously shown to give less accurate findings: the CSF compartment may accumulate compounds and reflect an averaged production and release, and repeated measures are difficult to obtain (Leoni and Caccia, 2011).

The secondary increase in 24-OHc levels was reported to result from neuronal loss and a wide release of molecules from the brain into the blood (Leoni and Caccia, 2011; Lütjohann et al., 2000). We showed an increase of the subiculum 24-OHc/CYP46A1 ratio for the patient who presented with hippocampal atrophy at brain examination, highlighting a focal neuronal death (Fig.3A). No increase was shown in both cortex (Fig.3B-C), possibly explained by the lack of cortical atrophy. We also reported increased 24-OHc levels for SE patients who were enrolled later after SE onset (Fig.3D-F). These patients presented with SE for several days; therefore, we may hypothesize that neuronal death had already begun.

This two-stage evolution of 24-OHc emphasizes the need of a precise timing of blood sampling, referred to SE onset to correctly interpret this variable (Fig.7). We can identify three periods: (1) first hours/days after SE onset, 24-OHc levels decrease; (2) several days after, 24-OHc levels normalize; (3) in patients and/or animals with sustained SE, suffering from secondary neuronal death, 24-OHc is finally released from the brain into the blood.

4.2. 24-OHc decreased levels are followed by an abnormal increase of cholesterol synthesis

The cholesterol synthesis and the 24-OHc production are closely related (Fig.7). Accordingly, we showed that decreased 24-OHc levels were associated with increased cholesterol levels.

Furthermore, we showed that increased cholesterol levels did not merely result from the blockage of the CYP46A1 enzymatic activity, but also resulted from an increase of the cholesterol synthesis. Desmosterol and cholesterol levels were higher in the subiculum of the patient who had the lowest 24-OHc/CYP46A1 ratio (Fig.4B). Increased cholesterol synthesis could reflect the lack of a negative feedback mechanism triggered by 24-OHc on the cholesterol synthesis enzymes (Boussicault et al., 2016; Chali et al., 2019; Leoni and Caccia, 2013). The activation of cholesterol enzymes by transcription-traduction occurred after several days, which could explain why only PSRSE patients presented with higher FC levels (Fig.5C, period 2 Fig.7C). A too early blood sampling does not measure the increase in the cholesterol synthesis (period 1 Fig.7C).

Two alternative pathways for cholesterol synthesis exist downstream of lanosterol: the Bloch and the Kandutsch-Russel pathway (Mitsche et al., 2015). Interestingly, we observed an increase of the cholesterol synthesis through two different pathways according to the compartment: (i) in brain, an increase of desmosterol levels both in human and mouse brains and in human CSF, through the Bloch pathway (Fig.4); and (ii) in the peripheral compartment, an increase of lanosterol and dihydrolanosterol levels in human plasma,

through the Kandutsch-Russel pathway (Fig.5F-G). Adult neurons essentially rely on astrocytes for cholesterol synthesis, which could explain the increase in the brain Bloch pathway activity. Altogether these data suggest that SE induces an abnormal increase of cholesterol synthesis in brain and in peripheral compartment.

4.3. Disturbances in peripheral cholesterol homeostasis and lipid transport

When low-density lipoprotein (LDL) particles are overloaded in the blood stream, lipids synthetized in the liver are transported thanks to ApoE/ApoB to the peripheral compartments. In contrast, high-density lipoprotein (HDL) particles transport cholesterol back to the liver after esterification by LCAT enzyme (Zhang and Liu, 2015). Brain transcripts for esterification enzymes increased persistently after SE onset in mice (Chali et al., 2019). However, we observed a decrease of serum EC and cholesterol esterification ratio in patients, which may result in a default to eliminate FC stored in peripheral compartments (Fig.5B).

After an injury, increased mobilization of cholesterol may be required for repair, growth and maintenance of myelin and neurons membranes (Wang et al., 2010). We observed increased sitosterol levels both in mouse hippocampi and human CSF. These data suggest that BBB is altered after SE and so, a cholesterol blood-brain handover could happen. We showed that PSRSE patients presented with the highest serum ApoE and ApoB levels, the lowest EC levels and the highest sitosterol CSF levels. We can speculate that the non-esterified cholesterol could be transported by apolipoproteins to the brain through an altered BBB (Fig.7).

Altogether, these data may suggest that cholesterol may be actively concentrated after SE. This may first be beneficial for the restoration of lipid membranes. On the other hand, in case of sustained SE, the excess of cholesterol may be excitotoxic for neuronal cells, as shown by the complete blockage of the CYP46A1 (Chali *et al*, 2015). The cholesterol accumulation could result in an increase of membrane viscosity and a decrease of neurotransmitter receptors mobility out of synapses, thereby increasing excitotoxicity and focal neuronal death. It may explain the neurologic sequels observed in SE patients and promote the use of cholesterol-lowering drugs that have previously shown their capability to reduce the association of NMDA receptor to lipid rafts in neuronal cultures, thereby decreasing the neurotoxicity (Ponce et al., 2008). Excitotoxicity could also be related to a direct regulation of numerous voltage-dependent and ligand-gated ion channels by cholesterol (Korinek et al., 2015; Paul et al., 2013).

In summary, our findings reveal disturbances in cholesterol homeostasis, similar in humans and in mouse model of SE, both in brain and in peripheral compartments (summarized in Fig.7A-B). The accumulation of cholesterol was previously shown to be responsible for neuronal death in animal models and in vitro. In this study, we demonstrated that SE induces an increase of the cholesterol synthesis both in humans and mice. Nevertheless, the prognosis significance of the increase of cholesterol synthesis remain to be explored in SE patients. If we demonstrate that disturbances of cholesterol homeostasis are associated with higher morbidity, the deleterious increase of brain cholesterol synthesis could be targeted by statins. Simvastatin has the highest BBB permeability (Sierra et al., 2011; Xie et al., 2011). Some studies conducted in rodents suggested a neuroprotective effect of simvastatin (Ponce et al., 2008; Xie et al., 2011; Zacco et al., 2003). Nonetheless, mechanisms underlying the neuroprotective effect of simvastatin are unknown (Omar et al., 2017; Quintana-Pájaro et al., 2018), and other studies did not report any effect (Funk et al., 2011; Trivedi et al., 2018).

Our study paves the way for research on statins as therapeutic intervention, in order to prevent the excitotoxicity and possibly subsequent neurological sequels of SE patients.

There are some limitations for this study: it was conducted in a single center, with various SE etiologies and treatments. Lumbar puncture was not performed for all patients and CSF was obtained more commonly for the patients with the most severe disease. Due to the smaller number of patients, we were not able to perform pairwise comparisons for CSF, and statistical analysis for the post-mortem samples. The interpretation of human post-mortem findings is limited by the small number of patients.

Nonetheless, the strengths of our study were the translational approach showing similar results for humans and KA mice, and the detailed analysis of lipid homeostasis by complementary methods. In addition, it was seemingly the first study demonstrating disturbances of cholesterol homeostasis in SE patients.

Author contributions

Name	Contribution
AH	Conceptualization, Methodology, Validation, Formal analysis, Investigation, Resources, Writing – Original draft, Writing – Review, Visualization, Supervision, Funding acquisition
PB	Methodology, Investigation, Resources, Visualization, Writing – Original draft
SD	Methodology, Investigation, Resources, Writing – Original draft
DR	Methodology, Investigation, Resources, Visualization, Writing – Original draft
SL	Methodology, Investigation, Resources, Visualization, Writing – Original draft
ET	Methodology, Investigation, Resources, Visualization, Writing – Original draft
MDa	Methodology, Investigation, Resources, Visualization, Writing – Original draft
DL	Methodology, Investigation, Resources, Visualization, Writing – Original draft
VL	Resources, Writing – Original draft
VF	Resources, Writing – Original draft
MDe	Resources, Writing – Original draft
IP	Resources, Writing – Original draft
DBR	Resources, Writing – Original draft, Supervision
RB	Methodology, Investigation, Resources, Writing – Original draft, Supervision
FL	Methodology, Investigation, Resources, Writing – Original draft, Supervision
VN	Conceptualization, Methodology, Validation, Formal analysis, Investigation, Resources, Writing – Original draft, Writing – Review, Visualization, Supervision, Funding acquisition

Study Group

Morgane Faure (Department of Pulmonology, Intensive Medicine and Resuscitation – R3S (SPMIR-R3S), Pitié-Salpêtrière Hospital, Paris, France), Bastien Herlin (Epileptology Unit, Pitié-Salpêtrière Hospital, France), Pierre Jaquet (Neuro-Intensive care Unit, Pitié-Salpêtrière Hospital, France), Clémence Marois (Neuro-Intensive care Unit, Pitié-Salpêtrière Hospital, France), Nicolas Mezouar (Epileptology Unit, Pitié-Salpêtrière Hospital, France), Benjamin Rohaut (Neuro-Intensive care Unit, Pitié-Salpêtrière Hospital, France), Nicolas Weiss (Neuro-Intensive care Unit, Pitié-Salpêtrière Hospital, France), Mark Williams (Department of Neurology, Yale School of Medicine, New Haven)

Declaration of competing interest

Aurélie Hanin reports no disclosure.

Paul Baudin reports no disclosure.

Sophie Demeret reports no disclosure.

Delphine Roussel reports no disclosure.

Sarah Lecas reports no disclosure.

Elisa Teyssou reports no disclosure.

Maria Damiano reports no disclosure.

David Luis reports no disclosure.

Virginie Lambrecq reports no disclosure.

Valerio Frazzini reports no disclosure.

Maxens Decavèle reports no disclosure.

Isabelle Plu reports no disclosure.

Dominique Bonnefont-Rousselot reports no disclosure.

Randa Bittar reports no disclosure.

Foudil Lamari reports no disclosure.

Vincent Navarro reports personal fees from UCB pharma, EISAI, GW Pharma and Liva Nova outside the submitted work.

Acknowledgements

The authors thank all the technical staff from the Histomics facility and from the PHENO-ICMice facility (Paris Brain Institute).

Funding sources

This work received support from the “Investissements d’avenir” program ANR-10-IAIHU-06, from the “Fondation pour la Recherche Médicale” (FDM20170839111) and from the Fondation Assitance Publique-Hôpitaux de Paris (EPIRES- Marie Laure PLV Merchandising).

All animal work was conducted at the PHENO-ICMice facility. The Core is supported by 2 “Investissements d’avenir” (ANR-10- IAIHU-06 and ANR-11-INBS-0011-NeurATRIS) and the “Fondation pour la Recherche Médicale”.

References

Bittar, R., Carrié, A., Nouadje, G., Cherfils, C., Fesel-Fouquier, V., Barbot-Trystram, L., Giral, P., Bonnefont-Rousselot, D., 2020. Evaluation of a semi-automatic isoelectric focusing method for apolipoprotein E phenotyping. Pract Lab Med 18, e00150. https://doi.org/10.1016/j.plabm.2019.e00150

Björkhem, I., Lütjohann, D., Diczfalusy, U., Ståhle, L., Ahlborg, G., Wahren, J., 1998. Cholesterol homeostasis in human brain: turnover of 24S-hydroxycholesterol and evidence for a cerebral origin of most of this oxysterol in the circulation. J. Lipid Res. 39, 1594–1600.

Björkhem, I., Meaney, S., 2004. Brain cholesterol: long secret life behind a barrier. Arterioscler. Thromb. Vasc. Biol. 24, 806–815. https://doi.org/10.1161/01.ATV.0000120374.59826.1b

Boussicault, L., Alves, S., Lamazière, A., Planques, A., Heck, N., Moumné, L., Despres, G., Bolte, S., Hu, A., Pagès, C., Galvan, L., Piguet, F., Aubourg, P., Cartier, N., Caboche, J., Betuing, S., 2016. CYP46A1, the rate-limiting enzyme for cholesterol degradation, is neuroprotective in Huntington's disease. Brain 139, 953–970. https://doi.org/10.1093/brain/awv384

Chali, F., Djelti, F., Eugene, E., Valderrama, M., Marquer, C., Aubourg, P., Duykaerts, C., Miles, R., Cartier, N., Navarro, V., 2015. Inhibiting cholesterol degradation induces neuronal sclerosis and epileptic activity in mouse hippocampus. Eur. J. Neurosci. 41, 1345–1355. https://doi.org/10.1111/ejn.12911

Chali, F., Milior, G., Marty, S., Morin-Brureau, M., Le Duigou, C., Savary, E., Blugeon, C., Jourdren, L., Miles, R., 2019. Lipid markers and related transcripts during excitotoxic neurodegeneration in kainate-treated mice. Eur. J. Neurosci. https://doi.org/10.1111/ejn.14375

Cuschieri, S., 2019. The STROBE guidelines. Saudi J Anaesth 13, S31–S34. https://doi.org/10.4103/sja.SJA_543_18

de Freitas, R.M., do Nascimento, K.G., Ferreira, P.M.P., Jordán, J., 2010. Neurochemical changes on oxidative stress in rat hippocampus during acute phase of pilocarpine-induced seizures. Pharmacol. Biochem. Behav. 94, 341–345. https://doi.org/10.1016/j.pbb.2009.09.015

Dietschy, J.M., Turley, S.D., 2004. Thematic review series: brain Lipids. Cholesterol metabolism in the central nervous system during early development and in the mature animal. J. Lipid Res. 45, 1375–1397. https://doi.org/10.1194/jlr.R400004-JLR200

Djelti, F., Braudeau, J., Hudry, E., Dhenain, M., Varin, J., Bièche, I., Marquer, C., Chali, F., Ayciriex, S., Auzeil, N., Alves, S., Langui, D., Potier, M.-C., Laprevote, O., Vidaud, M., Duyckaerts, C., Miles, R., Aubourg, P., Cartier, N., 2015. CYP46A1 inhibition, brain cholesterol accumulation and neurodegeneration pave the way for Alzheimer's disease. Brain 138, 2383–2398. https://doi.org/10.1093/brain/awv166

Funck, V.R., de Oliveira, C.V., Pereira, L.M., Rambo, L.M., Ribeiro, L.R., Royes, L.F.F., Ferreira, J., Guerra, G.P., Furian, A.F., Oliveira, Maurício Schneider, Mallmann, C.A., de Mello, C.F., Oliveira, Mauro Schneider, 2011. Differential effects of atorvastatin treatment and withdrawal on pentylenetetrazol-induced seizures. Epilepsia 52, 2094–2104. https://doi.org/10.1111/j.1528-1167.2011.03261.x

Hanin, A., Lambrecq, V., Denis, J.A., Imbert-Bismut, F., Rucheton, B., Lamari, F., Bonnefont-Rousselot, D., Demeret, S., Navarro, V., 2020. Cerebrospinal fluid and blood biomarkers of status epilepticus. Epilepsia 61, 6–18. https://doi.org/10.1111/epi.16405

Heverin, M., Bogdanovic, N., Lütjohann, D., Bayer, T., Pikuleva, I., Bretillon, L., Diczfalusy, U., Winblad, B., Björkhem, I., 2004. Changes in the levels of cerebral and extracerebral sterols in the brain of patients with Alzheimer's disease. J. Lipid Res. 45, 186–193. https://doi.org/10.1194/jlr.M300320-JLR200

Heverin, M., Engel, T., Meaney, S., Jimenez-Mateos, E.M., Al-Saudi, R., Henshall, D.C., 2012. Bi-lateral changes to hippocampal cholesterol levels during epileptogenesis and in chronic epilepsy following focal-onset status epilepticus in mice. Brain Res. 1480, 81–90. https://doi.org/10.1016/j.brainres.2012.08.018

Hirsch, L.J., Gaspard, N., van Baalen, A., Nabbout, R., Demeret, S., Loddenkemper, T., Navarro, V., Specchio, N., Lagae, L., Rossetti, A.O., Hocker, S., Gofton, T.E., Abend, N.S., Gilmore, E.J., Hahn, C., Khosravani, H., Rosenow, F., Trinka, E., 2018. Proposed consensus definitions for new-onset refractory status epilepticus (NORSE), febrile infection-related epilepsy syndrome (FIRES), and related conditions. Epilepsia 59, 739–744. https://doi.org/10.1111/epi.14016

Kim, J.-H., Jittiwat, J., Ong, W.-Y., Farooqui, A.A., Jenner, A.M., 2010. Changes in cholesterol biosynthetic and transport pathways after excitotoxicity. J. Neurochem. 112, 34–41. https://doi.org/10.1111/j.1471-4159.2009.06449.x

Korinek, M., Vyklicky, V., Borovska, J., Lichnerova, K., Kaniakova, M., Krausova, B., Krusek, J., Balik, A., Smejkalova, T., Horak, M., Vyklicky, L., 2015. Cholesterol modulates open probability and desensitization of NMDA receptors. J. Physiol. (Lond.) 593, 2279–2293. https://doi.org/10.1113/jphysiol.2014.288209

Le Duigou, C., Bouilleret, V., Miles, R., 2008. Epileptiform activities in slices of hippocampus from mice after intra-hippocampal injection of kainic acid. J. Physiol. (Lond.) 586, 4891–4904. https://doi.org/10.1113/jphysiol.2008.156281

Leoni, V., Caccia, C., 2013. 24S-hydroxycholesterol in plasma: a marker of cholesterol turnover in neurodegenerative diseases. Biochimie 95, 595–612. https://doi.org/10.1016/j.biochi.2012.09.025

Leoni, V., Caccia, C., 2011. Oxysterols as biomarkers in neurodegenerative diseases. Chem. Phys. Lipids 164, 515–524. https://doi.org/10.1016/j.chemphyslip.2011.04.002

Leoni, V., Mariotti, C., Tabrizi, S.J., Valenza, M., Wild, E.J., Henley, S.M.D., Hobbs, N.Z., Mandelli, M.L., Grisoli, M., Björkhem, I., Cattaneo, E., Di Donato, S., 2008. Plasma 24S-hydroxycholesterol and caudate MRI in pre-manifest and early Huntington's disease. Brain 131, 2851–2859. https://doi.org/10.1093/brain/awn212

Levitan, I., Singh, D.K., Rosenhouse-Dantsker, A., 2014. Cholesterol binding to ion channels. Front Physiol 5, 65. https://doi.org/10.3389/fphys.2014.00065

Lütjohann, D., Papassotiropoulos, A., Björkhem, I., Locatelli, S., Bagli, M., Oehring, R.D., Schlegel, U., Jessen, F., Rao, M.L., von Bergmann, K., Heun, R., 2000. Plasma 24S-hydroxycholesterol (cerebrosterol) is increased in Alzheimer and vascular demented patients. J. Lipid Res. 41, 195–198.

Marelli, C., Lamari, F., Rainteau, D., Lafourcade, A., Banneau, G., Humbert, L., Monin, M.-L., Petit, E., Debs, R., Castelnovo, G., Ollagnon, E., Lavie, J., Pilliod, J., Coupry, I., Babin, P.J., Guissart, C., Benyounes, I., Ullmann, U., Lesca, G., Thauvin-Robinet, C., Labauge, P., Odent, S., Ewenczyk, C., Wolf, C., Stevanin, G., Hajage, D., Durr, A., Goizet, C., Mochel, F., 2018. Plasma oxysterols: biomarkers for diagnosis and treatment in spastic paraplegia type 5. Brain 141, 72–84. https://doi.org/10.1093/brain/awx297

Martins, I.J., Berger, T., Sharman, M.J., Verdile, G., Fuller, S.J., Martins, R.N., 2009. Cholesterol metabolism and transport in the pathogenesis of Alzheimer's disease. J. Neurochem. 111, 1275–1308. https://doi.org/10.1111/j.1471-4159.2009.06408.x

Mitsche, M.A., McDonald, J.G., Hobbs, H.H., Cohen, J.C., 2015. Flux analysis of cholesterol biosynthesis in vivo reveals multiple tissue and cell-type specific pathways. Elife 4, e07999. https://doi.org/10.7554/eLife.07999

Noguchi, N., Saito, Y., Urano, Y., 2014. Diverse functions of 24(S)-hydroxycholesterol in the brain. Biochem. Biophys. Res. Commun. 446, 692–696. https://doi.org/10.1016/j.bbrc.2014.02.010

Noguchi, N., Urano, Y., Takabe, W., Saito, Y., 2015. New aspects of 24(S)-hydroxycholesterol in modulating neuronal cell death. Free Radic. Biol. Med. 87, 366–372. https://doi.org/10.1016/j.freeradbiomed.2015.06.036

Omar, A.S., Hanoura, S., Al-Janubi, H.M., Mahfouz, A., 2017. Statins in critical care: to give or not to give? Minerva Anestesiol 83, 502–511. https://doi.org/10.23736/S0375-9393.16.11493-2

Ong, W.-Y., Kim, J.-H., He, X., Chen, P., Farooqui, A.A., Jenner, A.M., 2010. Changes in brain cholesterol metabolome after excitotoxicity. Mol. Neurobiol. 41, 299–313. https://doi.org/10.1007/s12035-010-8099-3

Paul, S.M., Doherty, J.J., Robichaud, A.J., Belfort, G.M., Chow, B.Y., Hammond, R.S., Crawford, D.C., Linsenbardt, A.J., Shu, H.-J., Izumi, Y., Mennerick, S.J., Zorumski, C.F., 2013. The major brain cholesterol metabolite 24(S)-hydroxycholesterol is a potent allosteric modulator of N-methyl-D-aspartate receptors. J. Neurosci. 33, 17290–17300. https://doi.org/10.1523/JNEUROSCI.2619-13.2013

Paxinos, G., Watson, C., Pennisi, M., Topple, A., 1985. Bregma, lambda and the interaural midpoint in stereotaxic surgery with rats of different sex, strain and weight. J. Neurosci. Methods 13, 139–143.

Pokharel, S.M., Shil, N.K., Gc, J.B., Colburn, Z.T., Tsai, S.-Y., Segovia, J.A., Chang, T.-H., Bandyopadhyay, S., Natesan, S., Jones, J.C.R., Bose, S., 2019. Integrin activation by the lipid molecule 25-hydroxycholesterol induces a proinflammatory response. Nat Commun 10, 1482. https://doi.org/10.1038/s41467-019-09453-x

Ponce, J., de la Ossa, N.P., Hurtado, O., Millan, M., Arenillas, J.F., Dávalos, A., Gasull, T., 2008. Simvastatin reduces the association of NMDA receptors to lipid rafts: a cholesterol-mediated effect in neuroprotection. Stroke 39, 1269–1275. https://doi.org/10.1161/STROKEAHA.107.498923

Quintana-Pájaro, L.D.J., Ramos-Villegas, Y., Cortecero-Sabalza, E., Joaquim, A.F., Agrawal, A., Narvaez-Rojas, A.R., Moscote-Salazar, L.R., 2018. The Effect of Statins in Epilepsy: A Systematic Review. J Neurosci Rural Pract 9, 478–486. https://doi.org/10.4103/jnrp.jnrp_110_18

Ramirez, D.M.O., Andersson, S., Russell, D.W., 2008. Neuronal expression and subcellular localization of cholesterol 24-hydroxylase in the mouse brain. J. Comp. Neurol. 507, 1676–1693. https://doi.org/10.1002/cne.21605

Rossetti, A.O., Logroscino, G., Bromfield, E.B., 2006. A clinical score for prognosis of status epilepticus in adults. Neurology 66, 1736–1738. https://doi.org/10.1212/01.wnl.0000223352.71621.97

Rossetti, A.O., Lowenstein, D.H., 2011. Management of refractory status epilepticus in adults: still more questions than answers. Lancet Neurol 10, 922–930. https://doi.org/10.1016/S1474-4422(11)70187-9

Saeed, A.A., Genové, G., Li, T., Hülshorst, F., Betsholtz, C., Björkhem, I., Lütjohann, D., 2015. Increased flux of the plant sterols campesterol and sitosterol across a disrupted

blood brain barrier. Steroids 99, 183–188. https://doi.org/10.1016/j.steroids.2015.02.005

Sierra, S., Ramos, M.C., Molina, P., Esteo, C., Vázquez, J.A., Burgos, J.S., 2011. Statins as neuroprotectants: a comparative in vitro study of lipophilicity, blood-brain-barrier penetration, lowering of brain cholesterol, and decrease of neuron cell death. J. Alzheimers Dis. 23, 307–318. https://doi.org/10.3233/JAD-2010-101179

Sodero, A.O., Vriens, J., Ghosh, D., Stegner, D., Brachet, A., Pallotto, M., Sassoè-Pognetto, M., Brouwers, J.F., Helms, J.B., Nieswandt, B., Voets, T., Dotti, C.G., 2012. Cholesterol loss during glutamate-mediated excitotoxicity. EMBO J. 31, 1764–1773. https://doi.org/10.1038/emboj.2012.31

Solomon, A., Leoni, V., Kivipelto, M., Besga, A., Oksengård, A.R., Julin, P., Svensson, L., Wahlund, L.-O., Andreasen, N., Winblad, B., Soininen, H., Björkhem, I., 2009. Plasma levels of 24S-hydroxycholesterol reflect brain volumes in patients without objective cognitive impairment but not in those with Alzheimer's disease. Neurosci. Lett. 462, 89–93. https://doi.org/10.1016/j.neulet.2009.06.073

Trinka, E., Cock, H., Hesdorffer, D., Rossetti, A.O., Scheffer, I.E., Shinnar, S., Shorvon, S., Lowenstein, D.H., 2015. A definition and classification of status epilepticus--Report of the ILAE Task Force on Classification of Status Epilepticus. Epilepsia 56, 1515–1523. https://doi.org/10.1111/epi.13121

Trinka, E., Kälviäinen, R., 2017. 25 years of advances in the definition, classification and treatment of status epilepticus. Seizure 44, 65–73. https://doi.org/10.1016/j.seizure.2016.11.001

Trivedi, L.U., Alvarez, C.A., Mansi, I.A., 2018. Association of Statin Therapy With Risk of Epilepsy in 2 Propensity Score-Matched Cohorts. Ann Pharmacother 52, 546–553. https://doi.org/10.1177/1060028017756650

Wang, L., Han, Y., Chen, D., Xiao, Z., Xi, Z., Xiao, F., Wang, X., 2010. Cerebrospinal fluid apolipoprotein E concentration decreases after seizure. Seizure 19, 79–83. https://doi.org/10.1016/j.seizure.2009.12.001

Xie, C., Sun, J., Qiao, W., Lu, D., Wei, L., Na, M., Song, Y., Hou, X., Lin, Z., 2011. Administration of simvastatin after kainic acid-induced status epilepticus restrains chronic temporal lobe epilepsy. PLoS ONE 6, e24966. https://doi.org/10.1371/journal.pone.0024966

Yamanaka, K., Saito, Y., Yamamori, T., Urano, Y., Noguchi, N., 2011. 24(S)-hydroxycholesterol induces neuronal cell death through necroptosis, a form of programmed necrosis. J. Biol. Chem. 286, 24666–24673. https://doi.org/10.1074/jbc.M111.236273

Zacco, A., Togo, J., Spence, K., Ellis, A., Lloyd, D., Furlong, S., Piser, T., 2003. 3-hydroxy-3-methylglutaryl coenzyme A reductase inhibitors protect cortical neurons from excitotoxicity. J. Neurosci. 23, 11104–11111.

Zhang, J., Liu, Q., 2015. Cholesterol metabolism and homeostasis in the brain. Protein Cell 6, 254–264. https://doi.org/10.1007/s13238-014-0131-3

Figures legends

Fig.1: Flow chart of the study population

Fig.2: Time course of epileptic activities and neuronal death after kainate injection
(**A**) KA injection is followed by three periods: SE for 3 days, a latent period, and emergence of spontaneous seizures at 15 days. Mice were euthanized 1, 3, 7 or 15 days after injection. (**B**) Extract of an EEG of ipsilateral (right) and contralateral (left) hippocampus, from a KA mouse, at 1 day after the injection showing continuous polyspikes starting in the ipsilateral and spreading in the contralateral hippocampus (**up**), at 7 days showing interictal epileptiform discharges (**middle**) and at 15 days showing a spontaneous seizure followed by prolonged postictal depression with flattening of the EEG (**down**). Time frequency analysis of each EEG pattern is presented below the EEG extract. (**C**) NeuN (magenta) neuronal staining of the hippocampus shows a progressive reduction of neuronal density in CA1 region of KA injected mice at 7 days (D7) and 15 days (D15) in comparison with PBS injected mice and KA injected mice at 1 day (D1). Scale bar = 200µm. (**D**) Kinetics of disappearance of NeuN+ cells in CA1 region from the 1st day to the 15th day after intrahippocampal injection. Data are represented with the ratio of KA to PBS mice (mean ± SEM density; 5 animals; statistical analyses: Mann-Whitney test). The * indicates significant decrease (P=0.027) of the fluorescence intensity between D1 and D15.

Fig.3: Status epilepticus induces a decrease of 24-OHc levels both in humans and mice
(**A-C**) 24-OHc levels were measured respectively in the homogenates of subiculum from CONT (n=3) and SE patients (n=2) post-mortem tissues (**A**), lateral temporal cortex from CONT (n=8) and SE patients (n=2) post-mortem tissues (**B**) and frontal cortex from CONT (n=8) and SE patients (n=2) post-mortem tissues (**C**). Data were normalized by the concentration of the CYP46A1 in the extracts. (**D**) 24-OHc levels in the plasma of CONT and SE patients. Values of the different subgroups (FCONT, EPI, NRSE patients, RSE patients and PSRSE patients) are presented. We performed pairwise comparisons after a one-way

ANOVA test. (**E**) 25-OHc levels in the plasma of CONT and SE patients. Values of the different subgroups (FCONT, EPI, NRSE patients, RSE patients and PSRSE patients) are presented. We performed pairwise comparisons after a one-way ANOVA test. (**F**) 24-OHc plasma levels were correlated with the time between SE onset and blood sampling (days). The degree of correlation was evaluated with the Spearman test (rho 0.25; P=0.047). (**G**) 24-OHc levels were measured in both ipsilateral hippocampus (black bars) and contralateral hippocampus (grey bars) from mice at the four time points after KA injection (n=6-7 per time, per group). Data were normalized to those of PBS mice at each time. (**H**) Human paraffin post-mortem slices were stained with the monoclonal antibody against the CYP46A1 (blue). Strong expression was detected in the subiculum region, in which CYP46A1 staining was polarized and visible in the cell bodies and dendrites of pyramidal neurons, from both CONT and SE post-mortem tissues (**top**). Co-labelling of CYP46A1 and NeuN (magenta) immunostaining in hippocampus subiculum region shows a strong co-localization (**down**). No variation of intensity was found between CONT (n=2) and SE post-mortem patients (n=7). Scale bar=50 µm. (**I**) Examples of frozen post-mortem subiculum, lateral temporal cortex and frontal cortex from CONT and SE patients which were processed for western blotting with antibodies directed against CYP46A1 and GAPDH (**top**). Quantification of CYP46A1 levels normalized to GAPDH from CONT (n=3 and 8 respectively for subiculum and cortex) and SE patients (n=2) extracts (**down**).

All data are represented as mean ± SEM; statistical analyses: Student t test and Mann-Whitney test when appropriate. *P<0.05; **P<0.01; ***P<0.001 for NRSE patients or RSE patients *versus* CONT or KA-mice *versus* PBS-mice. #P<0.05 when compared with RSE patients.

Fig.4: Status epilepticus induces an abnormal increase in brain cholesterol synthesis.

(**A**) Schematic representation of the two enzymatic pathways for the conversion of squalene to cholesterol: Bloch and Kandutsch-Russel pathways, respectively shown on the left and on the right side. Sterols in bold were measured by UPLC-MS/MS. (**B, C and D**) Cholesterol and desmosterol levels were measured respectively in subiculum homogenates from CONT (n=3) and SE patients (n=2) post-mortem tissues (**B**), in homogenates of lateral temporal cortex from CONT (n=8) and SE patients (n=2) post-mortem tissues (**C**) and in homogenates of frontal cortex from CONT (n=8) and SE patients (n=2) post-mortem tissues (**D**). Data were normalized by the total protein concentration in the extracts. (**E-G**) Sterols were measured in the CSF of CONT patients and SE patients. (**H**) Desmosterol levels were

measured in both ipsilateral hippocampus (black bars) and contralateral hippocampus (grey bars) from KA injected mice at the four time points (n=6-7 per time, per group). Data were normalized to those of PBS mice at each corresponding time points. (**I**) Cholesterol levels were measured in both ipsilateral hippocampus (black bars) and contralateral hippocampus (grey bars) from mice at the four time points after KA injection (n=6-7 per time, per group). Data were normalized to those of PBS mice at each corresponding time points.

All data are represented as mean ± SEM; statistical analyses: Mann-Whitney test. *P<0.05; **P<0.01 for SE patients *versus* CONT or KA-mice *versus* PBS-mice.

Fig.5: Status epilepticus induces modifications in peripheral cholesterol homeostasis.

Total cholesterol (**A**) and esterified cholesterol (**B**) were measured in the serum of FCONT, EPI, NRSE patients, RSE patients and PSRSE patients. (**C**) Free cholesterol levels were correlated with the time between SE onset and blood sampling (days). The degree of correlation was evaluated with the Spearman test (rho 0.44; P=0.00030). (**D-E**) HDL-cholesterol levels were measured by enzymatic method (**D**) and levels were correlated with the triglyceride's concentration, in patients showing a hypertriglyceridemia (TG > 2.5 g/L). No correlation was observed using the Spearman test (rho -0.116; P=0.70) (**E**). (**F-H**) Lanosterol, dihydrolanosterol and desmosterol levels were measured in the plasma of FCONT, EPI, NRSE patients, RSE patients and PSRSE patients.

Data are represented as mean ± SEM; statistical analyses: Student t test and Mann-Whitney test when appropriate. *P<0.05; **P<0.01; ***P<0.001 when compared with FCONT or CONT. △P<0.05; △△P<0.01; △△△P<0.001 when compared with EPI. #P<0.05; ##P<0.01; ###P<0.001 when compared with RSE patients.

Fig.6: Blood – brain handover in status epilepticus

(**A**) CSF sitosterol levels were measured in SE patients and CONT. (**B**) Sitosterol levels were measured in both ipsilateral hippocampus (black bars) and contralateral hippocampus (grey bars) from KA injected mice at the two first time points (n=6-7 per time, per group). Data were normalized to those of PBS mice at each corresponding time points. (**C**) CSF ApoE levels were measured in CONT and SE patients. (**D**) Serum ApoE levels were measured in FCONT, EPI, NRSE patients, RSE patients and PSRSE patients. (**E**) ApoE phenotype: examples of isoforms of ApoE for eight patients, by isoelectric focusing gel, followed by immunoprecipitation on Hydragel 18 ApoE isofocusing. Results are indicated below the gel. (**F**) ApoE phenotype frequencies were determined for all FCONT, EPI and SE patients.

Data are represented as mean ± SEM; statistical analyses: Mann-Whitney test. *P<0.05; **P<0.01; ***P<0.001 when compared with CONT or FCONT. △△△P<0.001 when compared with EPI. #P<0.05 when compared with RSE patients.

Fig.7: Cholesterol homeostasis is modified in status epilepticus.

(**A**) Schema of cholesterol homeostasis regulation by the CYP46A1 in normal situation. 24-OHc controls the synthesis of cholesterol both in the brain and in the liver. Lipids synthetized in the liver are transported thanks to ApoE and ApoB to the peripheral compartments to be stored and used for biosynthesis. Free cholesterol must be esterified by LCAT enzyme to go back to the liver. (**B**) Cholesterol homeostasis is dysregulated in SE. Due to CYP46A1 inhibition, an increase of cholesterol synthesis occurs in the brain *via* the Bloch pathway stimulation and in the peripheral compartment *via* the Kandutsch-Russel pathway stimulation. The increase of serum apolipoprotein E (ApoE) could allow the transport of lipids from the liver into the brain *via* an altered blood-brain barrier. (**C**) Proposed time-evolution of free cholesterol (FC) and 24-OHc levels after SE. We distinguish three periods: (1) during the first hours/days after SE onset, we found a decrease of 24-OHc levels, probably related to the transitory CYP46A1 inhibition, and normal FC levels; (2) several days after SE onset, we showed increased FC levels due to the lack of negative feedback mechanism triggered by 24-OHc on the cholesterol synthesis enzymes and normalization of 24-OHc levels; (3) in case of sustained SE, patients or animals suffered from neuronal death which induces an increase of 24-OHc release.

Table 1: Clinical data from post-mortem patients

Patient : gender , age,	Group	Delay of brain examination post death, hours	Frozen tissues	Paraffin tissues	SE etiology	Cause of death	Prior history of epilepsy (Yes / No)	SE duration, days
1. m, 60	Control	18	Frontal Ctx Temporal Ctx	Frontal Ctx Temporal Ctx Hippocampus	-	Hemorrhagic shock	No	-
2. f, 66	Control	54	Frontal Ctx Temporal Ctx	Frontal Ctx Temporal Ctx	-	Multiorgan failure	No	-

				Hippocampus				
3. f, 66	Control	36	Frontal Ctx Temporal Ctx Hippocampus	Frontal Ctx Temporal Ctx Hippocampus	-	Pulmonary emboli	No	-
4. m, 66	Control	26	Frontal Ctx Temporal Ctx	-	-	Septic shock	No	-
5. m, 55	Control	48	Frontal Ctx Temporal Ctx	-	-	ARDS	No	-
6. f, 29	Control	32	Frontal Ctx Temporal Ctx Hippocampus	-	-	Septic Shock	No	-
7. m, 85	Control	Not precised	Frontal Ctx Temporal Ctx Hippocampus	-	-	Exacerbation of diabetes	No	-
8. f, 46	Control	17	Frontal Ctx Temporal Ctx	-	-	Multiorgan failure	Yes	-
1. m, 31	SE	22	Frontal Ctx Temporal Ctx Hippocampus	Frontal Ctx Temporal Ctx Hippocampus	NORSE	Withdrawal of life sustaining therapy	No	106
2. f, 27	SE	22	Frontal Ctx Temporal Ctx Hippocampus	Frontal Ctx Hippocampus	NORSE	Multiorgan failure	No	9
3. m, 70	SE	74	-	Frontal Ctx Temporal Ctx Hippocampus	NORSE	Not available	No	55
4. f, 56	SE	46	-	Frontal Ctx Temporal Ctx Hippocampus	AED withdrawal	Multiorgan failure	Yes	44
5. f, 39	SE	67	-	Frontal Ctx Temporal Ctx Hippocampus	NORSE	NORSE / Septic Shock	No	34
6. f, 41	SE	70	-	Frontal Ctx Temporal Ctx Hippocampus	NORSE	Not available	No	14
7. m, 29	SE	Not precised	-	Ammon's horn	Alcohol induced	Septic Shock	Yes	13
8. f, 70	SE	36	-	Frontal Ctx Hippocamp	Unknown	Pulmonary emboli	Yes	17

				us				

Abbreviations: AED = antiepileptic drug; ARDS = Acute Respiratory Distress Syndrome; f = female; m = male; NORSE = New-Onset Refractory Status Epilepticus; SE = status epilepticus

Table2: Biological and demographic characteristics of the study cohort.

Blood, N (%)	**63**	17 (27%)	26 (41%)	20 (32%)	**87**	43 (49%)	44 (51%)
Age, years [CI 95%]	**50.3 [45.6 – 54.9]**	59.1 [51.6 – 66.7]	50.2 [42.7 – 57.7]	42.8 [34.0 – 51.6]	**46.3 [42.2 – 50.3]**	53.7 [47.5 – 60.0]	39.0 [34.7 – 43.2]
Sex (m/f %)	**63**	71	73	45	**41**	47	36
ASAT/ALAT, AU [CI 95%]	**1.59 [1.24 – 1.94]**	2.40 [1.23 – 3.56]	1.49 [0.99 – 1.98]	1.14 [0.96 – 1.32]	**1.26 [1.11 – 1.41]**	1.17 [0.99 – 1.34]	1.40 [1.13 – 1.67]
Creatinine, µmol/L [CI 95%]	**72.3 [56.6 – 87.9]**	101.4 [46.9 – 155.7]	65.2 [56.0 – 74.3]	55.6 [42.8 – 68.4]	**71.2 [66.9 – 75.5]**	71.5 [66.0 – 77.0]	70.8 [63.4 – 78.1]
24-OHc, µg/L [CI 95%]	**37.2 [32.5 – 41.9]**	28.4 [23.6 – 33.2]	40.6 [32.7 – 48.5]	40.2 [30.3 – 50.2]	**44.2 [41.1 – 47.3]**	42.4 [37.9 – 46.9]	46.0 [41.7 – 50.3]
25-OHc, µg/L [CI 95%]	**23.8 [16.1 – 31.5]**	14.6 [11.0 – 18.2]	24.9 [17.3 – 32.5]	30.2 [7.58 – 52.9]	**18.8 [15.5 – 22.2]**	17.7 [12.5 – 22.8]	20.1 [15.6 – 24.5]
TC, g/L [CI 95%]	**1.59 [1.48 – 1.71]**	1.42 [1.19 – 1.65]	1.76 [1.58 – 1.94]	1.53 [1.34 – 1.72]	**1.94 [1.85 – 2.03]**	1.88 [1.74 – 2.02]	2.00 [1.88 – 2.12]
FC, g/L [CI 95%]	**0.60 [0.54 – 0.66]**	0.50 [0.38 – 0.63]	0.56 [0.51 – 0.62]	0.72 [0.57 – 0.86]	**0.57 [0.54 – 0.59]**	0.55 [0.52 – 0.58]	0.59 [0.55 – 0.62]
EC, g/L [CI 95%]	**1.01 [0.91 – 1.11]**	0.92 [0.75 – 1.08]	1.22 [1.08 – 1.36]	0.82 [0.62 – 1.02]	**1.37 [1.30 – 1.44]**	1.29 [1.19 – 1.38]	1.45 [1.35 – 1.55]
EC/TC, AU [CI 95%]	**0.62 [0.58 – 0.65]**	0.64 [0.60 – 0.69]	0.68 [0.65 – 0.70]	0.52 [0.42 – 0.61]	**0.70 [0.70 – 0.71]**	0.70 [0.69 – 0.71]	0.71 [0.70 – 0.72]
HDL-c, g/L [CI 95%]	**0.37 [0.32 – 0.42]**	0.45 [0.33 – 0.58]	0.42 [0.35 – 0.49]	0.23 [0.16 – 0.29]	**0.54 [0.51 – 0.58]**	0.53 [0.48 – 0.58]	0.56 [0.50 – 0.61]
TG, g/L [CI 95%]	**1.78 [1.39 – 2.17]**	1.25 [0.84 – 1.65]	1.45 [0.97 – 1.92]	2.67 [1.72 – 3.62]	**1.26 [1.09 – 1.44]**	1.31 [1.10 – 1.52]	1.21 [0.93 – 1.50]
ApoA1, g/L [CI 95%]	**1.05 [0.96 – 1.15]**	1.16 [0.92 – 1.41]	1.16 [1.05 – 1.26]	0.81 [0.66 – 0.96]	**1.42 [1.36 – 1.48]**	1.39 [1.30 – 1.47]	1.46 [1.37 – 1.54]
ApoB, g/L [CI 95%]	**0.92 [0.83 – 1.00]**	0.66 [0.53 – 0.79]	1.00 [0.86 – 1.13]	1.03 [0.89 – 1.17]	**0.94 [0.89 – 1.00]**	0.90 [0.83 – 0.97]	0.99 [0.90 – 1.07]
Lanosterol, µg/L [CI 95%]	**42.5 [30.3 – 54.7]**	24.7 [17.7 – 31.7]	38.5 [25.0 – 52.1]	61.7 [29.5 – 94.0]	**30.0 [19.9 – 39.6]**	27.7 [14.9 – 40.5]	31.5 [15.7 – 47.3]
Dihydrolanosterol, µg/L [CI 95%]	**19.0 [13.1 – 25.0]**	12.0 [-1.15 – 25.1]	13.7 [7.72 – 19.7]	29.5 [17.1 – 41.8]	**9.99 [8.19 – 11.8]**	9.49 [6.81 – 12.2]	10.4 [7.90 – 13.0]
Desmosterol, µg/L [CI 95%]	**362.6 [301.8 – 423.4]**	373.4 [132.5 – 614.3]	358.5 [294.4 – 422.5]	363.2 [218.2 – 508.1]	**425.9 [358.3 – 493.4]**	461.4 [350.8 - 572.0]	387.1 [309.2 – 465.0]
Sitosterol, µg/L [CI 95%]	**2309.4 [1154.6 – 3464.2]**	896.2 [-37.4 – 1829.9]	1018.7 [564.2 – 1473.1]	5580.8 [2018.7 - 9142.8]	**540.2 [448.9 – 631.5]**	524.0 [379.0 - 669.0]	558.1 [444.7 – 617.6]
ApoE, mg/dL [CI 95%]	**5.67 [5.00 – 6.34]**	5.00 [3.44 – 6.55]	4.92 [4.46 – 5.37]	7.31 [5.82 – 8.80]	**4.37 [4.06 – 4.68]**	4.22 [3.73 – 4.70]	4.51 [4.11 – 4.91]
CSF, N (%)	**32**	4 (12%)	13 (41%)	15 (47%)	**60**	43 (72%)	17 (28%)
Age, years [CI 95%]	**52.5 [45.8 – 59.2]**	57.0 [40.9 – 73.1]	58.2 [47.5 – 68.8]	46,4 [35.4 – 57.4]	**51.0 [45.9 – 56.0]**	53.7 [47.5 – 60.0]	43.9 [35.5 – 52.4]
Sex (M/F %)	**56**	100	69	33	**45**	47	41
24-OHc, µg/L [CI 95%]	**1.74 [1.55 – 1.94]**	1.60 [1.04 – 2.17]	1.72 [1.38 – 2.05]	1.80 [1.47 – 2.13]	**1.60 [1.49 – 1.70]**	1.61 [1.46 – 1.75]	1.57 [1.45 – 1.69]
Cholesterol, mg/L [CI 95%]	**2.36 [1.71 – 3.01]**	3.83 [-0.82 – 8.48]	1.94 [1.35 – 2.53]	2.44 [1.22 – 3.66]	**1.65 [1.22 – 2.07]**	1.42 [1.01 – 1.84]	2.19 [1.06 – 3.32]

Desmosterol, µg/L [CI 95%]	**2.38 [2.05 – 2.70]**	2.27 [2.19 – 2.34]	2.41 [1.95 – 2.87]	2.37 [1.77 – 2.97]	**1.82 [1.66 – 1.98]**	1.79 [1.60 – 1.98]	1.89 [1.56 – 2.21]
Lanosterol, µg/L [CI 95%]	**4.19 [0.29 – 8.09]**	<<	1.2	4.69 [0.09 – 9.30]	**2.51 [1.64 – 3.38]**	2.69 [1.59 – 3.80]	2.06 [0.32 – 3.79]
Dihydrolanosterol, µg/L [CI 95%]	**0.36 [0.09 – 0.62]**	<<	0.31 [0 – 0.63]	0.39 [-0.18 – 0.96]	**0.36 [0.30 – 0.43]**	0.35 [0.26 – 0.43]	0.41 [0.28 – 0.53]
Sitosterol, µg/L [CI 95%]	**3.53 [1.00 – 6.06]**	3.30 [-8.14 – 14.7]	1.21 [0.48 – 1.95]	5.20 [0.28 – 10.12]	**0.74 [0.52 – 0.97]**	0.69 [0.47 – 0.90]	0.89 [0.20 – 1.58]
Sitosterol diffusion CSF/(blood+CSF), AU [CI 95%]	**0.0073 [-0.0016 – 0.016]**	0.0063 [-0.062 – 0.074]	0.0042 [0 – 0.0086]	0.011 [-0.013 – 0.034]	**0.0040 [0 – 0.0073]**	0.0044 [0 – 0.0092]	0.0028 [0 – 0.0062]
ApoE, mg/dL [CI 95%]	**0.34 [0.29 – 0.40]**	0.35 [0.04 – 0.65]	0.32 [0.24 – 0.39]	0.36 [0.26 – 0.46]	**0.38 [0.34 – 0.42]**	0.40 [0.35 – 0.45]	0.33 [0.28 – 0.39]

Data are represented as percentages or mean [CI 95%].

Graphical abstract

Highlights

- Excitotoxic processes can follow a refractory status epilepticus (SE)
- SE induces CYP46A1 inhibition and a decrease of 24-OHc levels
- 24-OHc decreased levels is followed by an increase of cholesterol synthesis
- SE induces disturbances in cholesterol esterification and lipid transport
- Cholesterol is actively accumulated in brain after SE causing neuronal death